

Precision determination of the hyperfine-structure interval in the ground state of positronium. V

M. W. Ritter,* P. O. Egan,† V. W. Hughes, and K. A. Woodle
Gibbs Laboratory, Yale University, New Haven, Connecticut 06520
(Received 5 March 1984)

We report a new, more precise determination of the ground-state hyperfine-structure interval $\Delta\nu$ in positronium, which is based on extensive new data at low N_2 -gas densities combined with previous data from our group at Yale University. Our experimental value $\Delta\nu=203.389\,10(74)$ GHz (3.6 ppm) agrees with the current theoretical value $\Delta\nu=203.400$ GHz, for which the estimated uncertainty is about 50 ppm.

I. INTRODUCTION

Positronium (e^+e^-), often abbreviated by Ps, has been studied intensively in the past 30 years because it is a simple, basic leptonic atom.^{1,2} The electromagnetic interaction is dominant, and weak and hadronic interactions are negligibly small. The hyperfine structure interval $\Delta\nu$ in the ground state between orthopositronium (3S_1) and parapositronium (1S_0) is of fundamental importance for comparison of QED theory and experiment. This paper reports a new more precise measurement of $\Delta\nu$.

A history of the determinations³⁻¹¹ of $\Delta\nu$ is given in Table I. All of these determinations have been done by essentially the same experimental approach which has involved observation of the Zeeman transition in Ps and use of the Breit-Rabi equation to determine $\Delta\nu$. The magnetic field value used has been about 8–9 kG, and the mi-

crowave frequency required to induce the transition between the 3S_1 , $M=\pm 1$ and 3S_1 , $M=0$ states in the magnetic field was from 2.3 to 3.3 GHz. Observation of the transition is based on the change in the relative amount of 2γ and 3γ annihilation. The improvement in precision of determination of $\Delta\nu$ has come from the use of improved instrumentation for the magnetic field, microwave source, γ -ray detectors, and computer control as well as increased radioactive source strength; no important innovation in the basic experiment has been made. The series of experiments at Columbia and Yale^{5,6,9,10} will be designated Ps I–Ps IV, respectively. In the present paper, Ps V, we report additional improved measurements, particularly at low gas densities, and a determination of $\Delta\nu$ based on all the data of Ps IV and Ps V. An important correction to the theory of the line shape which includes relevant effects of the annihilation interaction is used.^{12,11}

The present theoretical value for $\Delta\nu$ is obtained from an approximate solution of the bound-state two-body relativistic equation and can be written¹³

$$\Delta\nu=203.4003+a(0.0108)-b(0.0021)\text{ GHz}, \quad (1)$$

where a and b have yet to be fully calculated. Expanded in powers of α we have

$$\Delta\nu=\alpha^2cR_\infty\left[\frac{7}{6}-\frac{\alpha}{\pi}\left(\frac{16}{9}+\ln 2\right)+\frac{5}{12}\alpha^2\ln\alpha^{-1}+a\frac{7}{6}\alpha^2-b\frac{\alpha^3}{\pi}(\ln\alpha^2)^2\right], \quad (2)$$

where $c=2.997\,924\,580(12)\times 10^{10}$ cm/s,¹⁴ $\alpha^{-1}=137.035\,963(15)$,¹⁵ and $R_\infty=1.097\,373\,152\,1(11)\times 10^5$ cm⁻¹.¹⁶ We note the lowest-order term which has not yet been fully calculated is of relative order α^2 or about 50 ppm. This accuracy is much poorer than the theoretical accuracy for $\Delta\nu$ of muonium (μ^+e^-). For Ps the calculations are more difficult because the masses of the e^- and the e^+ are the same and the particle-antiparticle annihilation process is present. When theoretical calculations of the coefficients a and b are completed, the theoretical error should be reduced to about 1 ppm.

Section II of this paper gives a brief overview of the experiment and a detailed discussion of our resonance line

TABLE I. Published values of the hyperfine-structure interval $\Delta\nu$ for the ground state of positronium.

Year	$\Delta\nu$ (GHz)	Error (ppm)
1952 ^a	203.2(3)	1500
1954 ^b	203.38(4)	200
1955 ^b	203.35(5)	250
1957 ^c	203.33(4)	200
1967 ^d	203.403(12)	58
1972 ^e	203.396(5)	24
1975 ^f	203.387 0(16)	8
1977 ^g	203.384(4)	20
1977 ^h	203.384 9(12)	6
1983 ⁱ	203.387 5(16)	8
1984 ^j	203.389 10(74)	3.6

^aDeutsch and Brown, Ref. 3.

^bWeinstein *et al.*, Ref. 4.

^cHughes *et al.*, Ref. 5.

^dTheriot *et al.*, Ref. 6.

^eCarlson *et al.*, Ref. 7.

^fMills and Bearman, Ref. 8.

^gCarlson *et al.*, Ref. 9.

^hEgan *et al.*, Ref. 10.

ⁱMills, Ref. 11.

^jThis paper.

shape. Section III describes the experimental apparatus. Section IV gives the data analysis including a discussion of errors. Section V gives our results together with a comparison with theory.

II. THEORY OF EXPERIMENT

The energy level diagram for the $n=1$ state of Ps is shown in Fig. 1. Our experiment involves the observation of the transition indicated whose frequency is given by the Breit-Rabi equation

$$f_0 = \frac{\Delta\nu}{2} [(1+x^2)^{1/2} - 1] \quad (3)$$

in which $x = (g'_- - g'_+) \mu_0 H_0 / h \Delta\nu$, $g'_+ (-) = g_+ (-) (1 - \frac{5}{24} \alpha^2)$ is the g factor for a positron (electron) in Ps,^{7,17} $g_+ / 2 = -[1 + 1.159652222(50) \times 10^{-12}]$, and $-g_+ / g_- = 1 + (22 \pm 64) \times 10^{-12}$,¹⁸ μ_0 is the Bohr magneton, H_0 is the static magnetic field, and h is Planck's constant. Corrections to this resonance frequency associated with Ps annihilation of relative order $(\lambda_p / 4\pi \Delta\nu)^2$ must be included. ($\lambda_p = 7.987 \times 10^9 \text{ s}^{-1}$ is the annihilation rate of 1S_0 Ps.¹³)

Positronium is formed in a static magnetic field H_0 when positrons from the ^{22}Na source are stopped and capture an electron in the N_2 gas in the microwave cavity. The $M=0$ level of 1S_0 Ps is mixed with the $M=0$ level of 3S_1 Ps in the field H_0 and hence the latter state annihilates into two γ rays with a lifetime of about 10 ns. The $M=\pm 1$ levels of 3S_1 Ps annihilate into three γ rays with a lifetime of about 140 ns. A microwave magnetic field H_1 of frequency f induces transitions between the $M=\pm 1$ levels and the $M=0$ level of 3S_1 Ps yielding an increase in two γ -ray annihilation which constitutes our experimental signal.

Our experimental line shape can be derived using the density matrix formalism for the Schrödinger equation. We use the angular momentum basis: $\psi_1 = |1,0\rangle$, $\psi_2 = |0,0\rangle$, $\psi_3 = |1,1\rangle$, and $\psi_4 = |1,-1\rangle$ where the quantum numbers in the kets stand for the total angular momentum J and its z projection M . The annihilation processes are represented as imaginary terms in the Hamiltonian.¹⁹ Off-resonance terms in the interaction with the microwave field are omitted.²⁰ The wave function is written $\psi(t) = \sum_j a_j(t) \psi_j$. Using the rotating coordinate basis with $a'_j(t) = e^{+i\omega_j t} a_j(t)$ where $\omega_1 = \omega_2 = \omega$ and $\omega_3 = \omega_4 = -\omega$, and $\omega \equiv 2\pi f$ where f is the microwave frequency,

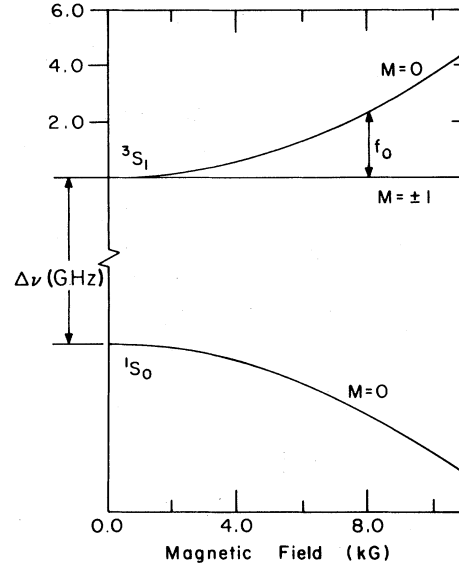


FIG. 1. Zeeman energy levels for ground-state Ps.

the effective time-independent Hamiltonian becomes²¹

$$\underline{R} = h \Delta\nu \begin{pmatrix} \Sigma_0 - \Omega/2 & x & 0 & 0 \\ x & \Sigma_p - \Omega/2 & -y & y \\ 0 & -y & \Sigma_0 + \Omega/2 & 0 \\ 0 & y & 0 & \Sigma_0 + \Omega/2 \end{pmatrix}, \quad (4)$$

where $\Sigma_p = E_p / (h \Delta\nu) - i\lambda_p / (4\pi \Delta\nu)$, $\Sigma_0 = E_0 / (h \Delta\nu) - i\lambda_0 / (4\pi \Delta\nu)$, E_p is the energy of *para*-Ps and E_0 is the energy of *ortho*-Ps at zero magnetic field, λ_p is the annihilation rate of *para*-Ps, and λ_0 is the annihilation rate of *ortho*-Ps, $y = (\sqrt{2}/2) H_1 (g'_- - g'_+) \mu_0 / (h \Delta\nu)$, and $\Omega = f / \Delta\nu$.

We use the density matrix Schrödinger equation in the form²²

$$\frac{d\vec{X}(t)}{dt} = 2\pi \Delta\nu \underline{C} \vec{X}(t). \quad (5)$$

\vec{X} is a 16-element column vector representing the density matrix

$$\begin{aligned} \vec{X}(t) = & \text{col}(\rho_{11}, \rho_{22}, \rho_{33}, \rho_{44}, \sqrt{\frac{1}{2}}(\rho_{12} + \rho_{21}), -i\sqrt{\frac{1}{2}}(\rho_{12} - \rho_{21}), \sqrt{\frac{1}{2}}(s^* \rho_{13} + s \rho_{31}), \\ & -i\sqrt{\frac{1}{2}}(s^* \rho_{13} - s \rho_{31}), \sqrt{\frac{1}{2}}(s^* \rho_{14} + s \rho_{41}), -i\sqrt{\frac{1}{2}}(s^* \rho_{14} - s \rho_{41}), \\ & \sqrt{\frac{1}{2}}(s^* \rho_{23} + s \rho_{32}), -i\sqrt{\frac{1}{2}}(s^* \rho_{23} - s \rho_{32}), \sqrt{\frac{1}{2}}(s^* \rho_{24} + s \rho_{42}), \\ & -i\sqrt{\frac{1}{2}}(s^* \rho_{24} - s \rho_{42}), \sqrt{\frac{1}{2}}(\rho_{34} + \rho_{43}), -i\sqrt{\frac{1}{2}}(\rho_{34} - \rho_{43})), \end{aligned} \quad (6)$$

where $\rho_{\alpha\beta} \equiv \langle \psi_\alpha | \psi(t) \rangle \langle \psi(t) | \psi_\beta \rangle$, $s = e^{i\omega t}$. \underline{C} is the 16×16 antisymmetric time-independent matrix representing the effective Hamiltonian,

$$\underline{C} = \begin{pmatrix} -\Gamma_0 & 0 & 0 & 0 & 0 & -\sqrt{2x} & 0 & 0 & 0 & 0 & 0 & 0 & 0 & 0 & 0 \\ 0 & -\Gamma_p & 0 & 0 & 0 & +\sqrt{2x} & 0 & 0 & 0 & 0 & 0 & -\sqrt{2y} & 0 & \sqrt{2y} & 0 & 0 \\ 0 & 0 & -\Gamma_0 & 0 & 0 & 0 & 0 & 0 & 0 & 0 & 0 & \sqrt{2y} & 0 & 0 & 0 & 0 \\ 0 & 0 & 0 & -\Gamma_0 & 0 & 0 & 0 & 0 & 0 & 0 & 0 & 0 & 0 & -\sqrt{2y} & 0 & 0 \\ 0 & 0 & 0 & 0 & -\Gamma_+ & 1 & 0 & -y & 0 & y & 0 & 0 & 0 & 0 & 0 & 0 \\ \sqrt{2x} & -\sqrt{2x} & 0 & 0 & -1 & -\Gamma_+ & y & 0 & -y & 0 & 0 & 0 & 0 & 0 & 0 & 0 \\ 0 & 0 & 0 & 0 & 0 & -y & -\Gamma_0 & -\Omega & 0 & 0 & 0 & x & 0 & 0 & 0 & 0 \\ 0 & 0 & 0 & 0 & y & 0 & \Omega & -\Gamma_0 & 0 & 0 & -x & 0 & 0 & 0 & 0 & 0 \\ 0 & 0 & 0 & 0 & 0 & y & 0 & 0 & -\Gamma_0 & \Omega & 0 & 0 & 0 & x & 0 & 0 \\ 0 & 0 & 0 & 0 & -y & 0 & 0 & 0 & -\Omega & -\Gamma_0 & 0 & 0 & -x & 0 & 0 & 0 \\ 0 & 0 & 0 & 0 & 0 & 0 & 0 & x & 0 & 0 & -\Gamma_+ & -1-\Omega & 0 & 0 & 0 & y \\ 0 & \sqrt{2y} & -\sqrt{2y} & 0 & 0 & 0 & -x & 0 & 0 & 0 & 1+\Omega & -\Gamma_+ & 0 & 0 & y & 0 \\ 0 & 0 & 0 & 0 & 0 & 0 & 0 & 0 & 0 & x & 0 & 0 & -\Gamma_+ & -1-\Omega & 0 & y \\ 0 & -\sqrt{2y} & 0 & \sqrt{2y} & 0 & 0 & 0 & 0 & -x & 0 & 0 & 0 & 1+\Omega & -\Gamma_+ & -y & 0 \\ 0 & 0 & 0 & 0 & 0 & 0 & 0 & 0 & 0 & 0 & 0 & -y & 0 & y & -\Gamma_0 & 0 \\ 0 & 0 & 0 & 0 & 0 & 0 & 0 & 0 & 0 & 0 & -y & 0 & -y & 0 & 0 & -\Gamma_0 \end{pmatrix} \quad (7)$$

where $\Gamma_0 = \lambda_0 / (4\pi \Delta\nu)$, $\Gamma_p = \lambda_p / (4\pi \Delta\nu)$, and $\Gamma_+ = \lambda_+ / (4\pi \Delta\nu)$ where $\lambda_+ = (\lambda_0 + \lambda_p) / 2$. We use the most recent theoretical values of the annihilation rates;¹³ ($^3S_1 \rightarrow 3\gamma$), $\lambda_0 = 7.0386 \times 10^6 \text{ s}^{-1}$ and ($^1S_0 \rightarrow 2\gamma$), $\lambda_p = 7.987 \times 10^9 \text{ s}^{-1}$.

The signal is proportional to the probability of 2γ annihilation,

$$P_{2\gamma} = \lambda_p \int_0^\infty \vec{Y}_p \cdot \vec{X}(t) dt \\ = \lambda_p \vec{Y}_p \cdot \underline{C}^{-1} \cdot \vec{X}(0) / (2\pi \Delta\nu). \quad (8)$$

Two γ annihilation is selected with the singlet-state projection operator $\vec{Y}_p = (0, 1, 0, \dots, 0)$; the initial state is taken to be unpolarized so that $\vec{X}(0) = \text{col}(\frac{1}{4}, \frac{1}{4}, \frac{1}{4}, \frac{1}{4}, 0, 0, \dots, 0)$. As indicated in the above discussion, in the Hamiltonian \underline{C} , only the atomic constant $\Delta\nu$ and H_1 are treated as unknowns. When H_0 and f are measured our data can be fitted to $P_{2\gamma}$ to determine $\Delta\nu$ as well as the microwave field H_1 . The numerical calculations based on Eq. (8) and discussed in Sec. IV were verified for the case $y=0$ by inverting the matrix \underline{C} by hand.

III. EXPERIMENTAL APPARATUS AND PROCEDURE

The apparatus used in this measurement is essentially the same as that used in Ps IV. The principal changes involved improved homogeneity and control of the static magnetic field and use of a stronger positron source.

A. Source

The positron source was 10–15 mCi of ^{22}Na , which is 2–3 times stronger than that used in Ps IV. The source capsule is made of oxygen-free high-conductivity Cu. A 0.0025-in.-thick Cu disk is soldered over the source to seal it. The source was delivered by New England Nuclear in 1978.

B. Gas handling system

The gas handling system is described in Ps III and Ps IV. In this experiment we evacuated our microwave cavity to a pressure of less than 5×10^{-6} Torr before each run. The cavity was then filled with 4–30 lbs/in.² (psi) of ultrapure N_2 gas (< 5 ppm contaminants). We concentrated our data taking at low N_2 pressures to reduce the necessary extrapolation to zero density.

C. Magnetic field

The magnet and its NMR system operate at about 7.8 kG and are described in Ps III and Ps IV. The magnet power supply was modified to accept a voltage produced by a digital-to-analog converter (DAC) to control and tune the magnetic field. The magnet was carefully shimmed to reduce the field inhomogeneity. The field was mapped before and after the experiment and no significant changes were found over the two-year period.

The NMR system used to stabilize and measure the magnetic field was substantially unchanged from Ps IV. An NMR probe⁹ filled with Nujol oil is connected to a fluxmeter to lock our magnetic field to a preset frequency, f_p (~ 33 MHz). The error voltage produced by the fluxmeter drives a current through a small coil placed over

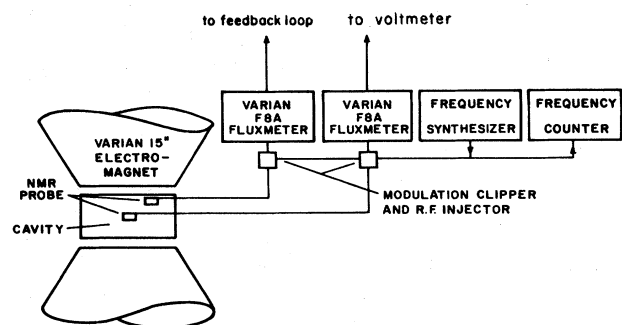


FIG. 2. Schematic diagram of the apparatus used to measure the magnetic field.

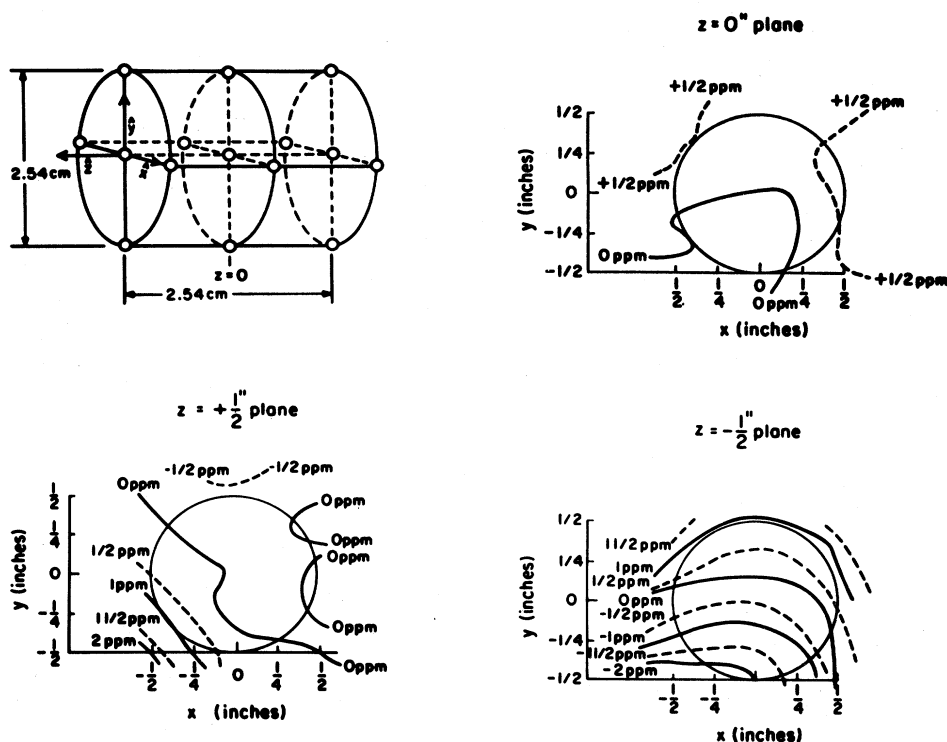


FIG. 3. Coordinate system and sample contour maps at $H_0 = 7.65$ kG.

the Hall probe normally used to stabilize the magnet.²³ The additional feedback allows the field to be locked with less than 0.3 ppm drift.

To map the magnetic field the cavity was removed and we used an additional probe and fluxmeter. Since both the locking probe and the measuring probe are driven at the same frequency, the error voltage produced by the second fluxmeter is proportional to the difference in the magnetic field at the two probe sites. The magnet was carefully mapped over the relevant volume where Ps 2γ annihilations are observed. Figure 3 shows typical field maps. The average of the magnetic field over this volume differed by less than 0.1 ppm from the value at the center of the microwave cavity.

With the cavity in place (Fig. 2) we measured the offset between the magnetic field at the locking site and at the center of the cavity. For the data analysis the average of the offset measurements at each field setting is used to correct the magnetic field values. Figure 4 shows offset measurements as a function of H_0 . To calibrate our fluxmeters we used an NMR probe (Varian Associates) filled with D_2O to lock the magnetic field to a different NMR frequency. In a locked field the error voltage produced as a function of the frequency, f_p , applied to the probes was found to be linear over the small (~ 25 ppm) ranges calibrated.

Corrections for diamagnetic and chemical shifts must be made to f_p . We measured the different NMR frequencies of our probes and of a cylindrical probe filled with H_2O and found that f_p must be raised by 3.6 ± 0.2 ppm. A further diamagnetic correction to f_p of -1.5 ± 0.1 ppm must be made to correct f_p to a standard spherical H_2O probe. We combine these two corrections with the best linear fit to our offset measurements

$$f'_p = f_p(1 - a \Delta f_p - b), \quad (9)$$

where f'_p is the NMR frequency of our probe at the center of the microwave cavity, $\Delta f_p \equiv f_p - f_c$, and f_c is the NMR frequency at the center of the resonance line, $a = 9.25(31)$ ppm/MHz and $b = 8.84(30)$ ppm. The direction of the magnetic field was the same throughout this experiment. No effect of the direction of the magnetic field on the determination of Δv has been observed in

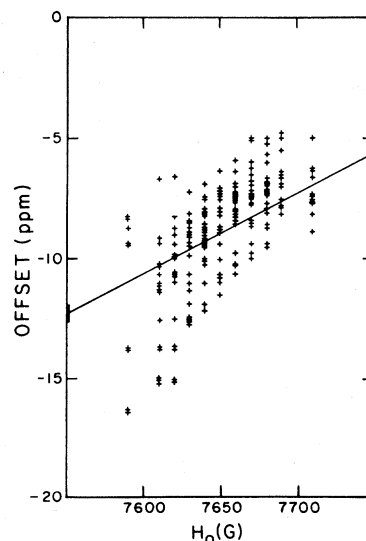


FIG. 4. Plot of all magnetic field offset measurements made. The offset is the difference between H_0 at the locking site and at the cavity center. The straight line is the best fit described in Eq. (9).

previous experiments^{6,8} which have used the coincident 2γ annihilation as the signal, and none is expected.

D. Microwaves

Our TM_{110} mode cavity is described in Ps III and the power generation and stabilization system in Ps IV. The microwave system produces a field H_1 with a frequency of 2.32 GHz and an amplitude of about 10 G (~ 300 W) in the x direction (with \vec{H}_0 in the z direction).

E. Detectors

The detectors and their associated electronics are described in Ps III and Ps IV; the photomultiplier tube gain stabilization system was not used. The four pairs of collinear detectors observe 0.5-MeV γ rays. Coincidences are counted by scalers in the CAMAC system.

F. Computer control

The experiment is automated through the CAMAC system described in Ps IV. The primary change has been to replace the precision stepping motor which controlled the magnetic field setting with a 12 bit DAC. The interrupt routines were rewritten for both the microwave power leveling and the magnet control which improved the reproducibility and reliability of the magnetic field settings.

G. Experimental procedure

Once the systems are turned on and have stabilized, data taking is controlled by the computer. The program steps and locks the field, levels the microwave power, and records the data at each magnetic field setting. Coincidences were counted for about 4 min at each field point. The magnetic field was swept back and forth from 7.6 to 8 kG. About 3 million counts are collected in a two-hour sweep over the resonance. Figure 5 shows a typical resonance line. About 300 resonance lines were observed in ten separate runs at nine different pressures.

IV. DATA ANALYSIS

The data analysis consists of two major steps. First, the data for each individual line are transferred to a Digital

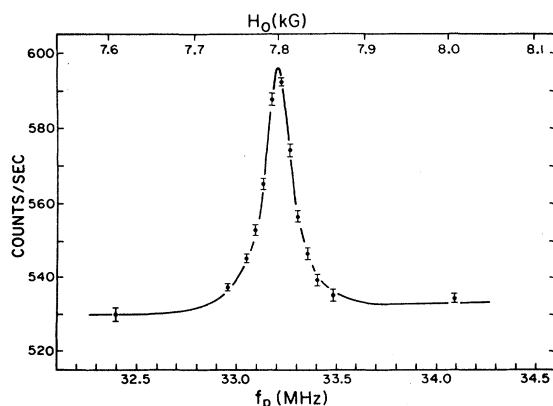


FIG. 5. Typical observed resonance line fit with the theoretical line shape of Eq. (11). These data were taken with 5.5 lbs/in.² (psi) of N_2 .

Equipment Corporation PDP-10 computer and fit as discussed below to determine $\Delta\nu(D)$. Second, the average value of $\Delta\nu(D)$ at the different gas densities D are fit to the linear equation

$$\Delta\nu(D) = \Delta\nu(1 + aD) \quad (10)$$

to obtain the extrapolated value $\Delta\nu$ at zero density.

The 2γ counting rate is given by

$$S = N_0(1 + m \Delta H)[(1 - r) + rP_{2\gamma}] \quad (11)$$

in which N_0 is a constant proportional to the strength of the e^+ source and to the detection efficiency, m is the background slope, r is the positronium formation fraction, H_c is the center of our resonance line, $\Delta H \equiv H_0 - H_c$, and $P_{2\gamma}$ is the probability that a ground-state unpolarized positronium atom will decay into two photons [Eq. (8)]. The background slope is primarily due to magnetic focusing of the positrons. $P_{2\gamma}$ involves the two unknown parameters $\Delta\nu$ and H_1 (see Sec. II). This formulation gives us five free parameters in our fits: $\Delta\nu$, H_1 , N_0 , m , and r . The quantity H_c is not an independent parameter. A typical fit is shown in Fig. 5 and determines the line center to about $\frac{1}{4}\%$ of the linewidth.

The computer time needed to process all of the lines using the complete density matrix formalism of Eqs. (8) and (11) is prohibitively long. We have processed some of the data with this full analysis. The majority of the data were analyzed by approximating $P_{2\gamma}$ by a Lorentzian function in Eq. (11); this approximation is designated S_L . We determine $\Delta\nu$ from the line center

$$\Delta\nu = \frac{1}{f} \left[\frac{g' \mu_B f_c}{2\mu_P} \right]^2 - f \quad (12)$$

using the Breit-Rabi equation where f_c is the NMR frequency at the center of the resonance line for a spherical water sample and $\mu_P'/\mu_B = 1.520992982(15) \times 10^{-3}$.¹⁴ Comparisons of the complete and approximate analyses in the cases where both were made indicates that only a small correction to $\Delta\nu$ of 0.7 ± 0.2 ppm needs to be made in the approximate analysis S_L .

We have also processed a selected portion of the data with the line shape used in Ps III and Ps IV, S_C . This line shape ignored off-diagonal matrix elements of the annihilation process in the Breit-Rabi eigenbasis and is therefore only accurate to ~ 10 ppm.¹² Use of either of the approximate line shapes S_L or S_C adds terms to the usual derivative of χ^2 proportional to

$$\sum_i \sum_j (S_i - S'_i) \frac{\partial S}{\partial \alpha_j} \Big|_i, \quad (13)$$

where the first sum is over the five parameters and the second sum is over the experimental points. S is the expected signal using the complete analysis while S' is either S_L or S_C . The quantity $S - S'$ is shown in Fig. 6. Since $\partial S / \partial \alpha$ is highly antisymmetric around the line center, the sum in Eq. (13) is quite small when S_L is used because

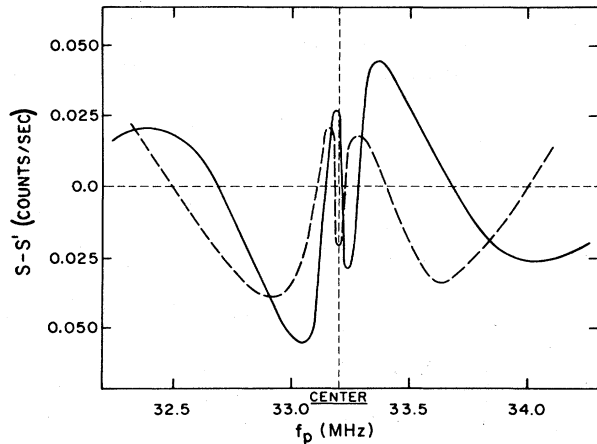


FIG. 6. Difference between the best fits of the approximations S' and the complete analysis S [Eq. (11)]. The solid line is $S - S_C$, while the dashed line is $S - S_L$.

$S - S_L$ is symmetric. In contrast $S - S_C$ is highly antisymmetric and the sum in Eq. (13) is large and hence leads to a significant systematic error in determining the line center. The value of $\Delta\nu$ derived using S_C must be increased by 18 ± 1 ppm, in rough agreement with Ref. 11.

For a given gas density D we determine $\Delta\nu(D)$ by averaging the values of $\Delta\nu$ obtained from the individual resonance lines. Figure 7 and Table II show the data from the present experiment and from Ps IV. In calculating the average for $\Delta\nu(D)$ we have discarded any line fits that had less than one percent chance of occurring according to χ^2 statistics. If we fit all of these data to Eq. (10), we obtain

$$\begin{aligned} \Delta\nu &= 203.389\,10(56) \text{ GHz (2.8 ppm)}, \\ a &= -3.3(4) \times 10^{-5} \text{ atm}^{-1} (0^\circ\text{C}), \end{aligned} \quad (14)$$

TABLE II. Measured values of $\Delta\nu$ at different N_2 -gas densities.

D [atm (at 0°C)]	$\Delta\nu$ (MHz)	σ (MHz)
	$\Delta\nu(D)$ 1983	
0.245	203 386.4	1.6
0.257	203 385.1	1.6
0.275	203 390.1	1.3
0.306	203 387.9	1.3
0.337	203 387.9	1.2
0.368	203 384.1	1.4
0.398	203 386.9	1.1
0.613	203 384.6	1.3
1.839	203 377.5	3.2
	$\Delta\nu(D)$ 1977	
0.251	203 386.3	2.0
0.314	203 387.6	1.4
0.377	203 385.1	1.6
0.439	203 386.9	2.5
0.565	203 386.9	2.6
0.628	203 381.8	2.0
0.941	203 382.1	2.0
1.260	203 385.3	4.0
1.880	203 372.9	3.5
2.510	203 370.1	4.9
2.820	203 371.6	2.9

where our χ^2 for the fit is 18.7 with 18 degrees of freedom; the error quoted is the statistical error only. The data were also fit with both a term linear in D and one quadratic in D ; the χ^2 fit was no better than that with the linear term alone and hence only the linear fit is used.

The sources of error in $\Delta\nu$ are listed in Table III. The errors for Ps IV are also shown. The principal error is due to counting statistics. The next largest error is due to the static magnetic field H_0 and is associated with the

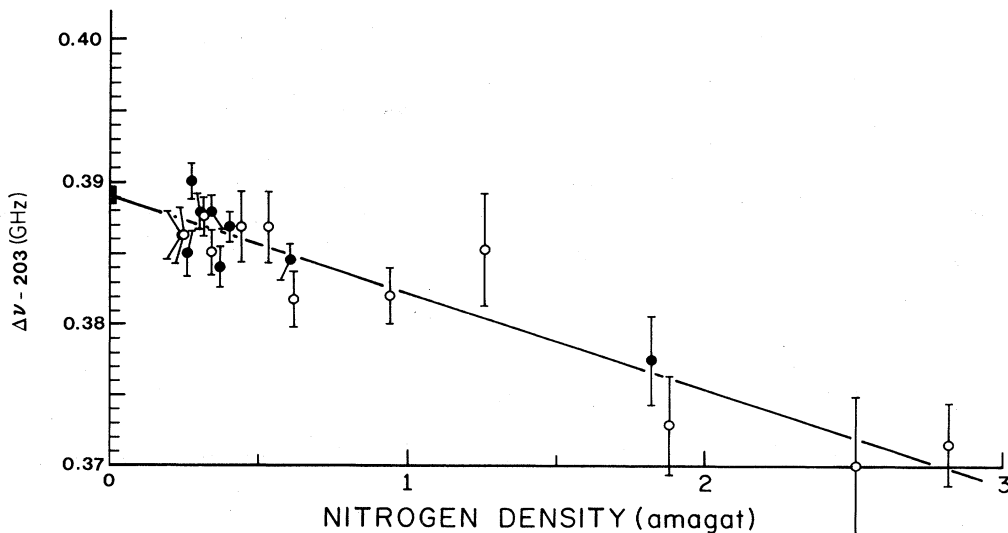


FIG. 7. Measured values of $\Delta\nu$ vs N_2 density (1 amagat is the density of 1 atm N_2 at 0°C). The open circles are from Ps IV and the closed circles are from the present work. The straight line is the best fit described in Eq. (14).

TABLE III. Uncertainties in $\Delta\nu$ measurement (ppm).

	1977	1983	All
Counting statistics	5.0	4.4	2.8
Magnetic field inhomogeneities	2.4	1.0	1.6
Magnetic field offset and reproducibility	1.4	0.8	1.0
Nuclear magnetic resonance (NMR) calibration	0.4	0.4	0.4
Microwave power and frequency uncertainty	0.5	0.5	0.5
Density uncertainty	0.3	0.3	0.3
Line-shape corrections	1.1	0.6	0.7
Quadrature sum	5.9	4.7	3.6

field inhomogeneity, the offset between the locking site and the active region, and the NMR calibration. Microwave power instability and uncertainty in the gas density and temperature account for smaller errors. Errors due to line-shape corrections include the Bloch-Siegert effect (0.5 ppm) (Ref. 22) and the approximations in the line-shape analysis described above (0.5 ppm weighted average for the data of Ps IV and of the present paper). Errors due to positron polarization (≤ 0.04 ppm), second-order magnetic interactions, and gas collisions are believed to be negligible.

The error due to magnetic field inhomogeneity occurs only due to the uncertainty of the spatial distribution of Ps. Using slits in front of the detectors we measured the 2γ annihilation rate as a function of position, which we take to be the Ps spatial distribution n :

$$n \propto (1 - \delta|x|)(1 - \delta|y|)(1 - \beta|z|) \quad (15)$$

where $\delta = 0.12 \text{ cm}^{-1}$ and $\beta = 0.4 \text{ cm}^{-1}$. The distribution function is normalized so that $n = 1$ at the origin. A good estimate of the error associated with the magnetic field inhomogeneity is the standard deviation of the field maps weighted by Eq. (15). This was found to be 0.5 ppm in H_0 which corresponds to 1 ppm in $\Delta\nu$. The field offset measurements shown in Fig. 4 were also fit to a straight line to determine that the maximum error in H_0 associated with the field offset is 0.4 ppm. Calibration of our NMR probe involved an error of 0.2 ppm.

The systematic errors associated with the microwave frequency measurement, microwave power instability, gas density, and temperature uncertainties are discussed in Ps IV. The effects of collisions are discussed in detail in Ps I and Ps II and should cause negligible error. For this paper a calculation was done which indicated that the measured variation of λ_0 with gas pressure shifted the value of $\Delta\nu$ by less than 0.04 ppm.

Since we combined all of the data to improve our fit we must also estimate the total systematic errors. A good estimate is obtained by averaging the systematic errors together weighted by the statistical errors. The total systematic error for the combined measurements of this paper and Ps IV is 2.1 ppm. For just the present measurement the total systematic error is 1.6 ppm as compared to 3.1 ppm for Ps IV.

V. RESULTS AND COMPARISON WITH THEORY

Our final result for $\Delta\nu$ is

$$\Delta\nu_{\text{expt}} = 203.389\,10(74) \text{ GHz} \quad (3.6 \text{ ppm}) \quad (16)$$

in which the 3.6 ppm is a one-standard-deviation error including the systematic and statistical errors. This value agrees with the latest value from Brandeis^{8,11} which is $\Delta\nu = 203.3875(16) \text{ GHz}$ (8 ppm). The combined best value is $\Delta\nu_{\text{expt}} = 203.388\,65(67) \text{ GHz}$ (3.3 ppm).

The current theoretical value is $\Delta\nu_{\text{theor}} = 203.4003 \text{ GHz}$. A complete calculation of the relative $O(\alpha^2)$ term has not been done so that an estimated error for $\Delta\nu_{\text{theor}}$ is 50 ppm. Within the relatively large theoretical error agreement of theory and our experiment is satisfactory,

$$\Delta\nu_{\text{theor}} - \Delta\nu_{\text{expt}} = 11.2 (\pm 10.8 \pm 0.7) \text{ MHz}, \quad (17)$$

where the first uncertainty is the estimated theoretical error and the second is the experimental error. Clearly additional theoretical calculations are required for comparison with experiment for this simplest lepton-antilepton atom.

Figure 8 shows the history of measured values of $\Delta\nu$. We note that the various values are in reasonable agreement. The only significant discrepancy is the 1977 Yale value for which the neglect of annihilation terms in the Hamiltonian produced a three-standard-deviation error.

The error in our present experimental value for $\Delta\nu$ cor-

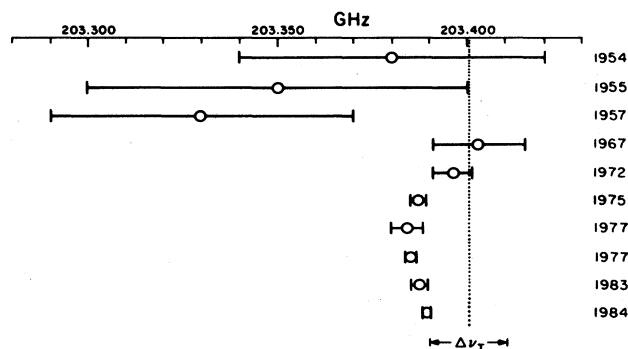


FIG. 8. Published values of $\Delta\nu$. The first measurement of $\Delta\nu$ (Ref. 3) is not plotted because of its relatively large quoted error. The dotted line together with its error bar gives the current theoretical value of $\Delta\nu$.

responds to choosing the center of the resonance line to one part in 2000. Although such an accuracy in choice of line center is not uncommon, it seems clear that some new line-narrowing technique is required for further substantial improvement in precision. Finally, we remark that a precision measurement of $\Delta\nu$ at zero magnetic field would be valuable, but appears very difficult because of the apparent requirements that the resonance line be obtained by sweeping the microwave frequency of about 203 GHz over the resonance line with fractional width of several parts in 10^3 , while maintaining constant microwave power.

ACKNOWLEDGMENTS

We would like to thank M. H. Yam for his help on early portions of the experiment and particularly for his work on the magnetic field. We would also like to acknowledge R. Broughton and S. Dhawan for their assistance with the electronics, C. J. Gardner for data taking, and G. Greene for computer programming. We gratefully acknowledge helpful discussions of the theory with P. Mohr and J. Sapirstein. This work was supported in part by National Science Foundation Grant No. PHY-81-08680.

*Present address: High Energy Physics Laboratory, Stanford University, Stanford, CA 94305.

†Present address: Lawrence Livermore National Laboratory, Livermore, CA 94550.

¹A. Rich, *Rev. Mod. Phys.* **53**, 127 (1981).

²V. W. Hughes, in *Precision Measurements and Fundamental Constants II*, edited by B. N. Taylor and W. D. Phillips, *Natl. Bur. Stand. (U.S.) Special Publication No. 617*, 1984, p. 237.

³M. Deutsch and S. C. Brown, *Phys. Rev.* **85**, 1047 (1952).

⁴R. Weinstein, M. Deutsch, and S. Brown, *Phys. Rev.* **94**, 758 (1954); **98**, 223 (1955).

⁵V. W. Hughes, S. Marder, and C. S. Wu, *Phys. Rev.* **106**, 934 (1957).

⁶E. D. Theriot, Jr., R. H. Beers, V. W. Hughes, and K. O. H. Ziock, *Phys. Rev. A* **2**, 707 (1970).

⁷E. R. Carlson, V. W. Hughes, M. L. Lewis, and I. Lindgren, *Phys. Rev. Lett.* **29**, 1059 (1972).

⁸A. P. Mills and G. H. Bearman, *Phys. Rev. Lett.* **34**, 246 (1975).

⁹E. R. Carlson, V. W. Hughes, and I. Lindgren, *Phys. Rev. A* **15**, 241 (1977).

¹⁰P. O. Egan, V. W. Hughes, and M. H. Yam, *Phys. Rev. A* **15**, 251 (1977).

¹¹A. P. Mills, *Phys. Rev. A* **27**, 262 (1983).

¹²A. Rich, *Phys. Rev. A* **23**, 2747 (1981).

¹³G. P. Lepage, in *Atomic Physics 7*, edited by D. Kleppner and F. M. Pipkin (Plenum, New York, 1981), p. 297; G. P. Lepage and D. R. Yennie, in *Precision Measurements and Fundamental Constants II*, edited by B. N. Taylor and W. D. Phillips, *Natl. Bur. Stand. (U.S.) Special Publication No. 617*, 1984, p. 237.

¹⁴E. R. Cohen and B. N. Taylor, *J. Phys. Chem. Ref. Data* **2**, 663 (1973).

¹⁵E. R. Williams and P. T. Olsen, *Phys. Rev. Lett.* **42**, 1575 (1979).

¹⁶S. R. Amin, C. D. Caldwell, and W. L. Lichten, *Phys. Rev. Lett.* **47**, 1234 (1981).

¹⁷H. Grotch and R. A. Hegstrom, *Phys. Rev. A* **4**, 59 (1971); M. L. Lewis and V. W. Hughes, *ibid.* **8**, 625 (1973).

¹⁸P. B. Schwinberg, R. S. Van Dyck, and H. Dehmelt, *Phys. Rev. Lett.* **47**, 1679 (1981).

¹⁹M. T. Grisaru, H. N. Pendleton, and R. Petrasso, *Ann. Phys. (N.Y.)* **79**, 518 (1973).

²⁰F. Bloch and A. Siegert, *Phys. Rev.* **57**, 522 (1940).

²¹G. T. Bodwin and D. R. Yennie, *Phys. Rep.* **43C**, 267 (1978); M. A. Stroschio, *ibid.* **22C**, 215 (1975).

²²A. P. Mills, *J. Chem. Phys.* **62**, 2646 (1975).

²³W. H. Wing, E. R. Carlson, and R. J. Blume, *Rev. Sci. Instrum.* **41**, 1307 (1970).